Synthesis of Bi_2O_3 Nanosheets and Photocatalysis for Rhodamine B

Wenwen ZHANG [1], Shaomin GAO [2], Donghui CHEN [1, 2 *]

[1] *College of Environmental Science and Engineering, Donghua University, Shanghai 201620, China*
[2] *College of Chemical and Environmental Engineering, Shanghai Institute of Technology, Shanghai 201418, China*

crossref http://dx.doi.org/10.5755/j01.ms.26.1.20494

Received 04 April 2018; accepted 24 July 2018

Bi_2O_3 nanosheets (NSB) photocatalyst was fabricated via a very simple method of liquid precipitation. The as obtained products were characterized by SEM, N_2 adsorption-desorption, XRD and UV-vis diffuse reflectance spectra. The results showed that NSB catalyst can beconsidered as set of nanosheets with an average thickness of 110 nm. NSB photocatalyst exhibited high surface area of 33.21 m^2/g and high purity. In addition, NSB catalyst displayed excellent photocatalytic performance for the dye of rhodamine B (Rh B) under visible light due to the structure of sheet and high surface area.
Keywords: Bi_2O_3, photocatalytic, nanosheets, Rh B.

1. INTRODUCTION

In recent years, based on in-depth research of waste water treatment technology, photocatalytic oxidation technology has drawn a lot of attention owing to its simple operation, high efficiency, good stability and no secondary pollution [1, 2]. However, the technology of photocatalytic oxidation in wastewater also has some drawbacks, for example, high cost, low utilization of natural light and material reuse. In this case, further research and developing of high activity photocatalytic materials is important.

With the development of nano science and technology, inorganic nano materials have obtained many researchers' attention because of their unique activities, such as small particle size, high surface area and surface energy [3, 4]. Inorganic nano materials have a special performance in the aspects of optical, electronic, and physical chemistry [4 – 7]. Up to now, inorganic nano materials with the morphology of particles, wires, rods, films, tubes, sheets et al have been researched. Among them, the nano materials with the morphology of sheet have attracted more and more researchers in photocatalytic field due to new characteristics including single crystal quality, high crystallinity, enhanced light absorption and separation efficiency of photo-generated charge carriers and other properties [8 – 10].

Bismuth, as one of the most abundant materials in China and all over the world, plays an important role in resource utilization with continuous development and utilization. Its oxide(Bi_2O_3) due to high dielectric constant, high refractive index, high oxygen ion conductivity, prominent photoconductivity and photoluminescence is widely used as a technically important material in the application of catalysis, chemical sensor and solid electrolyte materials [11 – 15]. From 1988, Harriman first proposed that Bi_2O_3 could be used as photocatalyst [16], more and more researches on Bi_2O_3 for the treatment of organic wastewater under light irradiation have been reported and Bi_2O_3 has been considered as one of the most promising photocatalyst due to its high oxygen vacancies, strong photoelectron and hole separation ability and high utilization of natural light [15, 17]. Up to now, Bi_2O_3 with the morphology of nanoparticles, spheres, flowers, nanoroads and fibers has been reported and applied in the field of photocatalycs [18 – 23]. Photocatalytic materials with nano-sheet morphology are beneficial for photocatalysis reaction because of superior properties. However, the researches about the nanosheet structure of Bi_2O_3 are not present.

This study intends to prepare NSB material by liquid precipitation method and compare it with commercial Bi_2O_3 with nanoparticle morphology (NPB). The photocatalytic activity through the degradation of Rh B solution under simulated visible light is studied.

2. MATERIALS AND METHODS

2.1. Materials

Materials were purchased from Shanghai Titan Scientific Co.,Ltd (China): bismuth(III) nitrate pentahydrate ($Bi(NO_3)_3{\cdot}5H_2O$, AR), nitric acid (HNO_3 AR), Hexamethylenetetramine ($C_6H_{12}N_4$, RG), ethanol (C_2H_5OH,AR), CB(AR), rhodamine B (Rh B). Deionized water (DI) supplied by our university was used in the experiments.

2.2. Synthesis of Bi_2O_3 nanosheets (NSB)

A simple method was successfully used to synthesize NSB. The preparation process was as follows: firstly, weighted 0.970 g $Bi(NO_3)_3{\cdot}5H_2O$ was dissolved in 20.0 mL HNO_3 solution (5.0 mL HNO_3 and 15.0 mL HO_2) in a single mouth flask with 40.0 mL HO_2. Then mixture solution was stirring at a suitable rate and heated to 70 ℃. Secondly, added 5.0 g $C_6H_{12}N_4$ (dissolved in 20.0 mL H_2O) and kept stirring and heating for 2.0 h. Finally, the suspension was centrifuged and washed with ethanol and water for two

* Corresponding author. Tel.: +84-021-6087328; fax: +84-021-6087328.
E-mail address: *chendhisit@163.com* (D. Chen)

times, respectively and dried at 70 ℃, then calcinated 2.0 h at 500 ℃ and the productions were gained.

2.3. Characterization

HITACHI S-3400N scanning electron microscope (SEM) was used to characterize the morphology of samples. A PANalytical X'Pert PRO X-ray diffractometer with Cu Ka (λ = 0.15418 nm) incident radiation was employed to analyze the crystal structure of the samples. Nitrogen adsorption and desorption experiments were performed at 77 K on a NOVA4000 gas adsorption analyzer (Quantachrome Corp.) to analyse the surface aero and pore size distribution. UV-Vis diffuse reflectance spectroscopy (UV-3600, Shimadzu, Japan) was used to examine the photo-physical properties of samples and the range of wavelenght was 200 – 800 nm. Photocatalytic activity of samples were determined by Beijing Purkinje General Instrument production of TU-1900.

2.4. Photocatalytic experiment

The photocatalytic performance of samples was evaluated by the decolorization rate studies of Rh B solution in a photochemical reactor (Beijing, China Education Au-light Co., Ltd). It was equipped with 300 W lamp as the visible light source, which was about 10 cm from the liquid surface of the suspensions. 60.0 mg samples were added in 100 mL 10 mg/L Rh B dye solution under constant magnetic stirring. Before lighting up, the suspension was stirred for 1.0 h in the condition of dark to reach the state of adsorption–desorption equilibrium. 4.5 mL suspensions was timely taken out and centrifuged for 4.0 min at the speed of 7000 r/min. The absorbance of the supernatant was measured by TU-1900 at 554 nm. The degradation rate *W* (%) was calculated according to the following formula:

$$W=(1 - At/Ao)\times 100\ \%, \quad (1)$$

where *Ao* and *At* are the absorbance of Rh B solution before light up and at the time of *t* after treatment.

3. RESULTS AND DISCUSSION

3.1. Morphology analysis

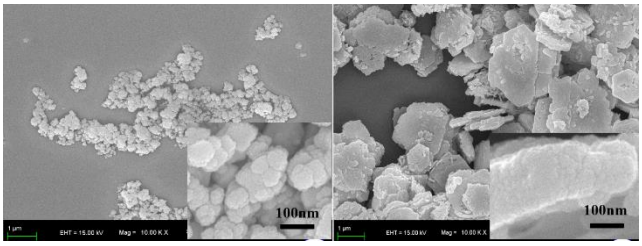

a b

Fig. 1. SEM images of: a – NPB; b – NSB

In order to analyze the morphology of samples, SEM was used. Fig. 1 displays the typical SEM images of NPB and NSB. It can be observed that the structure of as obtained sample NSB is nano-sheet with an average thickness of 110 nm in Fig. 1 b. NPB was nanoparticle shape with different size, whereas NSB consisted of smaller particles with the size around 40 – 60 nm (Fig. 1 a). NSB was formed through the aggregation of some smaller particles (Fig. 1 b), which may be caused by nanocrystals tend to shrink the exposed surface in order to reduce the surface energy [24]. From Fig. 1 b it is easily to find that the surface of NSB is rough and has some holes that will be beneficial to increase the surface area.

3.2. XRD analysis

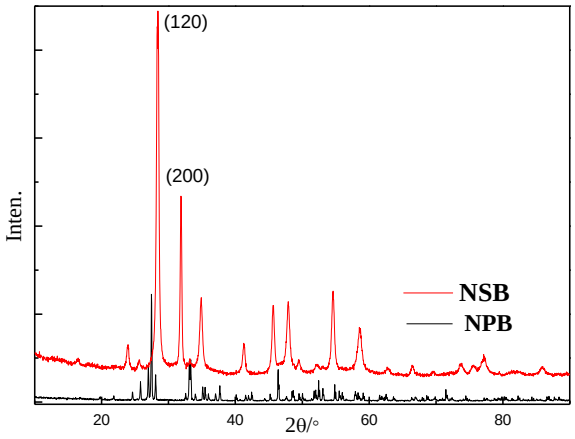

Fig. 2. XRD patterns of NPB and NSB

Bi_2O_3 possess distinct crystalline structures and physical properties which due to the four polymeric forms (a-δ-Bi_2O_3, β-δ-Bi_2O_3, γ-δ-Bi_2O_3 and δ-Bi_2O_3) [25]. The crystalline phases of the as obtained product was identified by XRD patterns. Fig. 2 depicts all the diffraction peaks of NPB and NSB. According to JCPDS files (No. 41–1449, No.71-2274 and No.27-0050), both NSB and NPB are not single phase Bi_2O_3. Moreover, the peaks of NSB are more narrow and sharp and no peaks of other materials are found, that indicates that the purity of NSB is better.

3.3. Surface area analysis

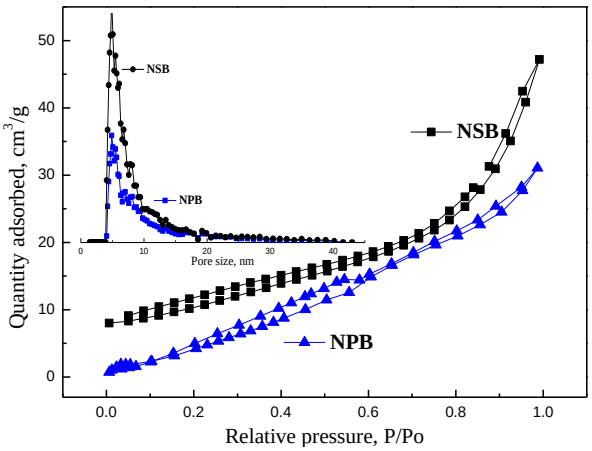

Fig. 3. Nitrogen adsorption-desorption isotherms and the pore size distribution of samples (the inset)

Large surface area is beneficial to adsorb more reactants on the surface of the catalyst and high pore volume is useful for various reactants and products spread rapidly in photocatalytic catalytic reaction process, and then improve the photocatalytic activity and degrade organics more quickly [26]. So, it is meaningful to analyze the surface area and pore volume of samples. Fig. 3 presents the nitrogen adsorption-desorption isotherms and corresponding pore

size distribution curves (inset) of NSB and NPB. From the data of nitrogen adsorption-desorption isotherms, the surface area of NSB could be reached to 33.21 m^2/g whereas NPB is just 27.56 m^2/g. According to the IPUAC classification, the isotherm plot reveals that NSB and NPB belong to the porous materials [27]. According to Fig. 3 the pore size of NSB and NPB are mainly distributed in 5 – 10 nm and the proportion of NSB is much more than NPB. Fig. 3 reveals that NSB have an advantage over NPB in the field of photocatalytic because of the larger surface area and higher proportion of pores.

3.4. Optical properties

The photo-physical properties of synthesized NSB were studied by UV–vis DRS spectroscopy. Fig.4 exhibits the typical UV–vis diffuse reflectance spectra of NPB and NSB. By contrast, it is clearly noted that, both of them set out good absorption below the wavelength of 400 nm and low absorption above 600 nm. Nevertheless, the absorption of NSB is stronger than NPB in all region. High absorption for visible light demonstrates that the material is suitable for photocatalysis. As a crystallite semiconductor, the optical absorption near the band edge follows the equation:

$$\alpha h\nu = C\left(h\nu - E_g\right)^{1/2}, \qquad (2)$$

where *a*, *v*, *Eg* and *C* are the absorption coef-ficient, light frequency, band gap, and a constant respectively [28]. The *Eg* of Bi_2O_3 could be estimated from a plot of $(ahv)^2$ versus photo energy (*hv*) [29]. As shown in Fig. 4 b, the *Eg* of NSB and NPB are found to be 2.27 eV and 2.32 eV, indicating that NSB have stronger absorption and higher photocatalytic activity than NPB under visible light.

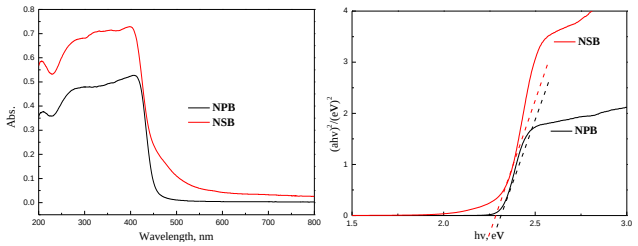

a b

Fig. 4. UV-vis diffuse reflectance spectra: a – NSB and NPB; b – energy band gap of NSB

3.5. Catalyst activity

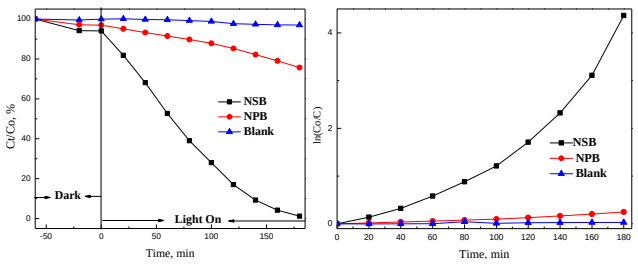

a b

Fig. 5. Photocatalytic activity of samples under visible light irradiation: a – degradation rate of Rh B; b – relationship between ln(C_0/C) and irradiation time of Rh B

The photocatalytic activity of samples can be evaluated by the degradation rate of Rh B solution. Fig. 5 presents the photocatalytic activity of samples under visible light irradiation. Fig. 5 a presents that Rh B solution can be degraded in the condition of visible light after adding the samples. Before turning on the light, it is obviously observed that the concentration of Rh B solution with nothing is almost stay the same. Moreover, the concentration of Rh B solution with NSB and NPB is decreased a little. Comparing the data during darkness, the samples could reach the state of adsorption equilibrium in 30 min and the adsorption ability of NSB is better than NPB, which may be caused by the high surface area. After turning up the light, the concentration of blank control also stays the same in 1.0 h and then decreases with time. 3.0 h later, the blank control is totally decreased about 3.1 %. However, the concentration of solution with NPB and NSB have been decreasing over time. Lighting for 1.0 h, the concentration of solution with NPB and NSB is degraded to 52.6 % and 91.4 %. After lighting up 3.0 h, the degradation of solution with NSB almost reached to 98.8 % and the NPB was just 24.4 %. The relationship between ln(C_0/C) and irradiation time of the degradation by NPB and NSB is shown in Fig. 5 b, where C_0 and C are the concentration before and after lighting on, respectively. It is quite obvious that the relationship of the degradation with NSB is not linear and the photodegradation with NSB exhibits auto-accelerated effect. That reveals that the photodegradation with NPB does not follow the reaction kinetics of pseudo-first-order, which may be cased by the intermediate products produced during degradation effect the conditions and enhance the photocatalytic activity of NSB [30]. It could be obtained that the photocatalytic property of NSB with the unique morphology is better than NPB [8 – 10].

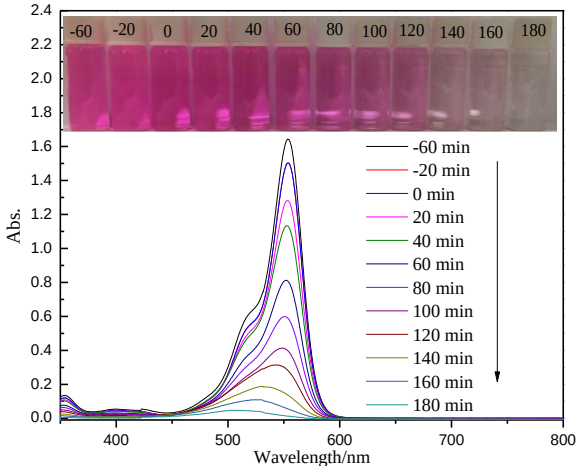

Fig. 6. UV-vis absorption spectra and the color changes photo images of Rh B

In order to clearly view the degradation of Rh B solution, UV-visible absorption spectra and the photos about color change were used. It is easy to view these changes in Fig. 6. The color of Rh B solution is more and more light and 3.0 h later, it almost becomes transparent, indicating Rh B solution has been degraded completely. The intensity of the absorption peak at the wavelength of 554 nm, which represents the concentration of Rh B solution, rapidly decreased with time and accompanied by a

gradual blue shift of the absorption band, indicating that demethylation of Rh B occurs during the oxidation reaction [31]. 3.0 h later, the characteristic absorption peaks of Rh B almost completely disappeared, implying that the dye of Rh B is almost completely degraded. Therefore, it is concluded that NSB has excellent photocatalytic activity under visible light irradiation.

4. CONCLUSIONS

In summary, NSB with an average thickness of 110 nm was synthesized by one step method of liquid precipitation. The photocatalytic performance of NSB was investigated. Compared with NPB, the as-prepared NSB material not only displayed higher surface area (33.21 m^2/g) and purity, but also exhibited excellent photocatalytic activity by the degradation of Rh B that could be reached to 91.4 % which was higher than CNB (52.6 %) upon visible light irradiation. That could be due to the morphology of nano-sheet that improves the visible light absorption and electron–hole separation efficiency. This paper provides a simple method for the preparation of good photocatalyst and demonstrates that NSB could be a promising photocatalyst in the field of water treatment.

REFERENCES:

1. **He, Y.J., Sutton, N.B., Rijnaarts, H.H., Langenhoff, A.M.** Degradation of Pharmaceuticals in Wastewater using Immobilized TiO_2, Photocatalysis under Simulated Solar Irradiation *Applied Catalysis B Environmental* 189 2016: pp. 283 – 283. https://doi.org/10.1016/j.apcatb.2015.09.015
2. **Huang, Y., Sun, F., Wu, T., Wu, Q., Zhong, H., Su, H., Zhang, Z.** Photochemical Preparation of CDS Hollow Microspheres at Room Temperature and Their Use in Visible-light Photocatalysis *Journal of Solid State Chemistry* 184 (3) 2011: pp. 644 – 648. https://doi.org/10.1016/j.jssc.2011.01.012
3. **Zhang, W., Chen, D.** Preparation and Performance of CeO_2 Hollow Spheres and Nanoparticles *Journal of Rare Earth* 34 (3) 2016: pp. 295 – 299. https://doi.org/10.1016/S1002-0721(16)60028-5
4. **Mario, G.J., Rosana, F.G., Kellen, C.M.B., Murillo, H.M. R., M, R.B.D.** Functional Nanomaterials for Applications in Energy Storage and Conversion, American Scientific Publishers, Los Angeles 2009. pp. 217-237. https://doi.org/10.1007/978-3-319-53898-3_9
5. **Bodson, D.** Nanoparticles and Nanostructured Films, Wiley-VCH 1988. http://dl.merc.ac.ir/handle/Hannan/4708
6. **Kim, K., Lee, J.W., Lee, H.B., Shin, K.S.** Novel Fabrication of Au Nanoparticle Films on Planar and Curved Surfaces of Glass and Fiber Materials *Langmuir the ACS Journal of Surfaces & Colloids* 25 (17) 2009: pp. 9697 – 9702. https://doi.org/10.1021/la9009465
7. **Pourfath, M., Kosina, H.** Encyclopedia of Nanoscience and Nanotechnology 1 – 10 (9) 2006: pp. 541 – 581. https://pubs.acs.org/doi/pdf/10.1021/cen-09136-ad11
8. **Li, B., Shao, L., Zhang, B., Wang, R., Zhu, M., Gu, X.** Understanding Size-dependent Properties of BiOCl Nanosheets and Exploring More Catalysis *Journal of Colloid & Interface Science* 505 2017: pp. 653 – 663. https://doi.org/10.1016/j.jcis.2017.06.060
9. **Nair, A.K., Jagadeeshbabu, P.E.** Ag-TiO_2 Nanosheet Embedded Photocatalytic Membrane For Solar Water Treatment *Journal of Environmental Chemical Engineering* 5 (4) 2017: pp. 4128 – 4133. https://doi.org/10.1016/j.jece.2017.07.046
10. **Omomo, Y., Sasaki, T., Wang, L., Watanabe, M.** Redoxable Nanosheet Crystallites of MnO_2 Derived Via Delamination of a Layered Manganese Oxide *Cheminform* 125 (12) 2003: pp. 3568 – 3575. https://doi.org/10.1002/chin.200324215
11. **Leontie, L., Caraman, M., Alexe, M., Harnagea, C.** Structural and Optical Characteristics of Bismuth Oxide thin Films *Surface Science* 507 2002: pp. 480 – 485. https://doi.org/10.1016/S0039-6028(02)01289-X
12. **Fruth, V., Ramer, R., Popa, M., Calderon-Moreno, J.M., Anghel, E.M., Gartner, M.** Deposition and Characterization of Bi_2O_3, Thin Films on Different Substrates *Journal of Materials Science Materials in Electronics* 18 (1) 2007: pp. 187 – 190. https://doi.org/10.1007/s10854-007-9207-7
13. **Fan, H.T., Teng, X.M., Pan, S.S., Ye, C., Li, G.H., Zhang, L.D.** Optical Properties of δ-Bi_2O_3 Thin Films Grown by Reactive Sputtering *Applied Physics Letters* 87 (23) 2005: pp. 231916 – 231919. https://doi.org/10.1063/1.2136351
14. **Sammes, N.M., Tompsett, G.A., Näfe, H., Aldinger, F.** Bismuth Based Oxide Electrolytes – Structure and Iionic Conductivity *Journal of the European Ceramic Society* 19 (10) 1999: pp. 1801 – 1826. https://doi.org/10.1016/s0955-2219(99)00009-6
15. **Shuk, P., Wiemhöfer, H.D., Guth, U., Göpel, W., Greenblatt, M.** Oxide Ion Conducting Solid Electrolytes Based on Bi_2O_3 *Solid State Ionics* 89 (3 – 4) 1996: pp. 179 – 196. https://doi.org/10.1016/0167-2738(96)00348-7
16. **Harriman, A., Thomas, J.M., Zhou, W., Jefferson, D.A.** A New Family of Photocatalysts Based on Bi_2O_3 *Journal of Solid State Chemistry* 72 (1) 1988: pp. 126 – 130. https://doi.org/10.1016/0022-4596(88)90015-1
17. **Cheng, H., Huang, B., Lu, J., Wang, Z., Xu, B., Qin, X., Zhang, X., Dai, Y.** Synergistic Effect of Crystal and Electronic Structures on the Visible-light-driven Photocatalytic Performances of Bi_2O_3 Polymorphs *Physical Chemistry Chemical Physics* 12 (47) 2010: pp. 15468 – 15475. https://doi.org/10.1039/C0CP01189D
18. **Cheng, L., Kang, Y.** Cheminform Abstract: Selective Preparation of Bi_2O_3, Visible light-driven Photocatalyst by Dispersant and Calcination *Cheminform* 585 (6) 2014: pp. 85 – 93. https://doi.org/10.1002/chin.201406017
19. **Qin, F., Qin, F., Li, R., Wang, W. J., Sun, H., Chen, R.** Template-free Fabrication of Bi_2O_3 and $(BiO)_2CO_3$, Nanotubes and their Application in Water Treatment *Cheminform* 18 (51) 2012: pp. 16491 – 16497. https://doi.org/10.1002/chem.201201989
20. **Schlesinger, M., Schulze, S., Hietschold, M., Mehring, M.** Metastable β-Bi_2O_3 Nanoparticles with High Photocatalytic Activity from Polynuclear Bismuth Oxido Clusters *Dalton Transactions* 42 (4) 2013: pp. 1047 – 1056. https://doi.org/10.1039/C2DT32119J
21. **Liang, Z., Cao, Y., Li, Y., Xie, J., Guo, N., Jia, D.** Solid-State Chemical Synthesis of Rod-like fluorine-doped β-Bi_2O_3 and their Enhanced Photocatalytic Property Under Visible Light *Applied Surface Science* 390 2016: pp. 78 – 85.

https://doi.org/10.1016/j.apsusc.2016.08.085

22. **Brezesinski, K., Ostermann, R., Hartmann, P., Perlich, J., Brezesinski, T.** Exceptional Photocatalytic Activity of Ordered Mesoporous β-Bi_2O_3 Thin Films and Electrospun Nanofiber mats *Chemistry of Materials* 22 (22) 2010: pp. 3079 – 3085. https://doi.org/10.1021/cm903780m
23. **Bagheri, M., Heydari, M., Vaezi, M.R.** Influence of Reaction Conditions on Formation of Ionic Liquid-based Nanostructured Bi_2O_3 as an Efficient Visible-light-driven Photocatalyst *Journal of Physics & Chemistry of Solids* 112 2017: pp. 14 – 19. https://doi.org/10.1016/j.jpcs.2017.08.020
24. **Du, N., Zhang, H., Chen, B., Xiangyang, M.A., Yang, D.** Ligand-free Self-assembly of Ceria Nanocrystals into Nanorods by Oriented Attachment at Low Temperature *Journal of Physical Chemistry C* 111 (34) 2007: pp. 12677 – 12680. https://doi.org/10.1021/jp074011r
25. **Leontie, L., Caraman, M., Delibaş, M., Rusu, G.I.** Optical Properties of Bismuth Trioxide Thin Films *Materials Research Bulletin* 36 (9) 2001: pp. 1629 – 1637. https://doi.org/10.1016/s0025-5408(01)00641-9
26. **Li, B., Shao, L., Zhang, B., Wang, R., Zhu, M., Gu, X.** Understanding Size-dependent Properties of BiOCl Nanosheets and Exploring more Catalysis *Journal of Colloid & Interface Science* 505 2017: pp. 653 – 663. https://doi.org/10.1016/j.jcis.2017.06.060
27. **Zhang, J., Wang, Y., Yu, C., Shu, X., Jiang, L., Cui, J., Chen, Z., Xie, T., Wu, Y.** Enhanced Visible-light Photoelectrochemical Behaviour of Heterojunction Composite with **C**u_2O Nanoparticles-decorated TiO_2 Nanotube Arrays *New Journal of Chemistry* 38 (10) 2014: pp. 4975 – 4984. https://doi.org/10.1039/C4NJ00787E
28. **Fu, H., Yao, W., Zhang, L., Zhu, Y.** The Enhanced Photoactivity of Nanosized Bi_2WO_6 Catalyst for the Degradation of 4-chlorophenol *Materials Research Bulletin* 43 (10) 2008: pp. 2617 – 2625. https://doi.org/10.1016/j.materresbull.2007.10.044
29. **Chen, R., Shen, Z., Wang, H., Zhou, H., Liu, Y., Ding, D., Chen, T.** Fabrication of Mesh-like Bismuth Oxide Single Crystalline Nanoflakes and Their Visible Light Photocatalytic Activity *Journal of Alloys & Compounds* 509 (5) 2011: pp. 2588 – 2596. https://doi.org/10.1016/j.jallcom.2010.11.102
30. **Deng, W., Chen, D., Hu, J., Chen, L.** A General and Green Approach to Synthesize Monodisperse Ceria Hollow Spheres with Enhanced Photocatalytic Activity *RSC Advances* 5 (98) 2015: pp. 80158 – 80169. https://doi.org/10.1039/C5RA15602E
31. **Wang, D.H., Wang, L., Xu, A.W.** Room-temperature Synthesis of Zn(0.8) Cd(0.2)S Solid Solution with a High Visible-light Photocatalytic Activity for Hydrogen Evolution *Nanoscale* 4 (6) 2012: pp. 2046 – 2053. https://doi.org/10.1039/c2nr11972b